ISSN 2176-5480

22nd International Congress of Mechanical Engineering (COBEM 2013)
November 3-7, 2013, Ribeirão Preto, SP, Brazil

STUDY OF FRACTURE IN WELDED JOINT OF A STEEL API 5L X80 USING ACOUSTIC EMISSION TECHNIQUE

Waldemir dos Passos Martins
IFMA – Institute Federal of Maranhão. Campus São Luís – Monte Castelo. Av.Getúlio Vargas, nº. 04. Monte Castelo. São Luís-MA. CEP: 65030-005.
waldemir@ifma.edu.br

Antonio Ernandes Macedo Paiva
IFMA – Institute Federal of Maranhão. Campus São Luís – Monte Castelo. Av.Getúlio Vargas, nº. 04. Monte Castelo. São Luís-MA. CEP: 65030-005.
ernandes@ifma.edu.br

Valdemar Silva Leal
IFMA – Institute Federal of Maranhão. Campus São Luís – Monte Castelo. Av.Getúlio Vargas, nº. 04. Monte Castelo. São Luís-MA. CEP: 65030-005.
vs.leal@uol.com.br

Valtair Antonio Ferraresi
UFU – University Federal of Uberlândia. Av.João Naves de Ávila 2121 - Campus Santa Mônica. CX 593. Uberlândia – MG. CEP 38408-100.
valtairf@mecanica.ufu.br

Abstract. *This work presents an investigation of the initial stage of formation and crack propagation hydrogen in welded joints in steel API 5L X80, using the test implant and technique of acoustic emission (AE). To this end, we developed a device called acoustic emission "Acoustic Emission System - AES" and a computer program to record the acoustic signals generated by the events of the crack. Welds were made used as the filler metal cored wire ER110-MC with 1.2 mm diameter as shielding gas mixtures Ar + 25% CO_2 and Ar + 25% CO_2 + 3% H_2, and the results of trials related to modes of fracture observed. This technique provided a unique opportunity to monitor the kinetics of crack and to assess the intensity of the process of cracking, with the results providing a basis for studies on the phenomenon of hydrogen cracking in welding of high strength steels.*

Keywords: *Hydrogen crack, API X80 Steel, Acoustic emission, Implant test.*

1. INTRODUCTION

Despite the significant progress in the development of high-strength and low-alloy (HSLA) steel, to improve their weldability and welding consumables with low hydrogen potential, cold cracking or hydrogen cracking is still the biggest problem in welding production. For many years the hydrogen crack has been considered as a typical defect of heat affected zone (HAZ) of welded joints of structural steels. With the introduction of new high-strength steels obtained from the controlled rolling followed by accelerated cooling and high carbon reduction, the hydrogen crack has been considered as a relevant problem in the HAZ and a major problem in the fusion zone (FZ) (Widgery, 2002).

In these steels, depending on the microstructure of the metal, the diffusible hydrogen concentration and weld residual stress level, the risk of hydrogen crack arises when cooling of the weld reaches the temperature of 150°C to -100°C. Generally, the crack hydrogen occurs late and may appear up to 48 hours after the welding. Usually, hydrogen cracks are located near the HAZ or FZ (Nevasmaa, 2003). Thus, to assess whether a material is susceptible or not to hydrogen cracking, a large number of tests have been developed several decades ago for understanding and characterization of various forms of cracks which may occur in a weld, since the occurrence of these is a complex event that depends on numerous aspects and many of them are difficult to characterize (Boellinghaus, *et al*., 2010).

Of the various types of tests developed some provide only qualitative results (like "crack / no crack"). Other tests provide quantitative results, however, in most cases, these results can not directly be used to predict whether cracks may be formed during the actual welding of a structure. Among the various types of tests, highlight the trials where tensions arise from the assembly itself, this type of test is commonly called the **Self-restricted test or Direct test**, including, for example, the test Tekken, GBOP test, CTS test and WIC test. These tests enable a quick assessment of the full joint (FZ and HAZ) by counting the number of cracks for each body of proof (BP), but depend on the level of restriction imposed and the form of the chamfer and weld bead. The trials in which the request is imposed by an external device that applies a load or strain controlled on BP, during or after welding, are known as **Tests with external constraints or Indirec**t, including implant test, CLR test, RRC test, TRC test and ASC test . Indirect tests, in general, are characterized by being conducted in BPs carved under load or constant strain (Boellinghaus, *et al*., 2010).

ISSN 2176-5480

However, it is apparent that only with the use of susceptibility testing proposed we do not guarantee that their answers may extend for actual practical applications, and it became necessary to find another tool, together with the susceptibility tests mentioned above, could contribute more information. One possibility was the use of the technique of Acoustic Emission (AE). As non-destructive evaluation techniques, the method of acoustic emission (AE) has been widely used in recent decades to inspect nuclear plants, bridges and fuel tanks due to their ability to monitor in real time. Since the acoustic emission is highly sensitive to some specific and localized micro events, for example, the movement of dislocations, initiation, growth and multiplication of micro cracks and cracking interfacial, the AE method is useful in identifying the origin, the magnitude and source distribution that generates this event characteristic. When evaluating the mechanical / metallurgical welds, although there are significant advances in investigations of AE, other experimental and theoretical studies are still needed to achieve a better understanding of the relationship between the behavior of the AE and this behavior of the steel. Until now there has been no systematic investigation of the behavior of EA in welds of steel API X80 (Lee, *et al*.,1999).

Hippsley et al. (1988) revealed that, if there was a sudden change in the internal stress field in a material, caused for instance by the propagation of a crack of slip band, then some of the stored elastic energy was dissipated as elastic wave (stress waves). Depending on their amplitude, these could be detected as AE by piezoelectric sensors attached to the surface of the material. Broadly speaking, the amplitude of the detected AE depends on the size and duration of each deformation or fracture event. Furthermore, AE is only emitted when a crack advances, and not when it remains static. Thus careful measurements of the emission activity as a function of time or stress, for instance, can be used to give insights into the dynamics of fracture. Consequently the present study is aimed was developed an acoustic emission equipment, called "Acoustic Emission System – AES" and DELPHI computer program to record the acoustic signals generated by the events of the crack, which coupled to the implant test allowed a deeper analysis of the event the initiation and propagation of a hydrogen crack. Thus, the aim of this study was to investigate the initiation of crack hydrogen in welded joints of API x80 steel using the acoustic emission technique.

2. EXPERIMENTAL PROCEDURE

2.1. Materials

The chemical composition and mechanical properties of the API X80 steel used in the study are given in Tab.1. The plates allocation implants and thermocouples had dimensions of 330 mm x 200 mm x 20 mm (length x width x thickness), as shown in Fig.1a. For the fabrication of implants, we used samples from plates similar to the BP, taken in the rolling direction and prepared according to standard AFNOR NF A89-100, with the welds of implants performed in the same direction. "The reason for using implants with the same material of plates is not to have variation of the thermal conductivity of these components."

Table 1. Chemical composition and mechanical properties of the steel.

Chemical Composition (wt %)										
C	**Si**	**Mn**	**P**	**S**	**Al**	**Cu**	**Nb**	**V**	**Ti**	**Cr**
0,05	0,29	1,81	0,017	0,001	0,020	0,02	0,069	0,033	0,020	0,17
Ni	**Mo**	**Sn**	**N**	**As**	**B**	**Ca**	**Sb**	**-**	C_{eqIIW}	P_{cm}
0,01	0,21	0,001	0,0034	0,003	0,0002	0,0012	0,00		0,44	0,18
Propriedades Mecânicas										
Yield Strength (YS) MPa			**Tensile Strength (TS) MPa**			**Elongation (ε) %**			**Hardness HV**	
660			741			26			250	

The plates for allocation the implants, Fig.1b, were machined to remove the surface oxide layer and pierced with ten (10) holes of 6.5 mm diameter corresponding allocating ten (10) implants and ten (10) holes of diameter 2.5 mm, for allocation of thermocouples, which are equally spaced holes for a total of ten (10) tests per plate. Fig.2b shows the schematic drawing the dimensions of the implant. As filler metal was used solid wire AWS 5.18 ER 70S-6 and flux cored wire AWS 5.28 E 110 MC, diameter 1.2 mm and as shielding gas the gas mixtures Ar + 25% CO_2 and Ar + 25% CO_2 + 3% H_2. The addition of 3% H_2 in Ar + 25% CO_2 aimed to induce high levels of diffusible hydrogen in the weld pool and thus create the conditions suitable for cracking by hydrogen. The chemical composition and mechanical properties of the filler metals are shown in Tab.2. The carbon equivalent shown in Tab.1 and Tab.2 were determined by eq.(1) by Ito, Bessyo and eq.(2) of IIW (International Institute of Welding).

$$Ceq\ (Pcm) = C + Si/30 + Mn/20 + Cu/20 + Ni/60 + Cr/20 + Mo/15 + V/10 + 5B \quad (1)$$

$$Ceq\ (IIW) = C + Mn/6 + (Cr + Mo + V)/5 + (Ni + Cu)/15 \quad (2)$$

ISSN 2176-5480

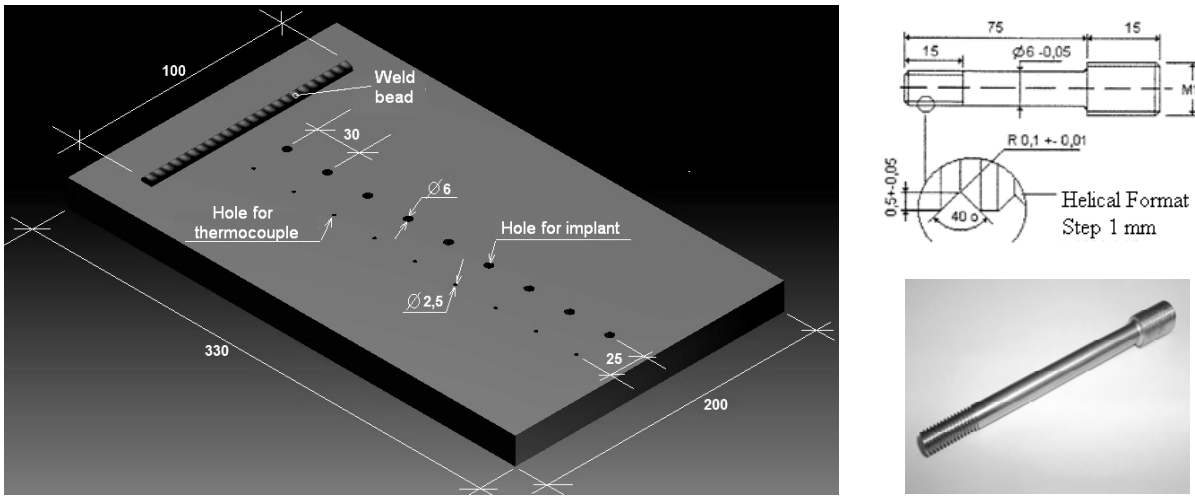

(a) (b)

Figure 1. (a) Schematic representation of the BP with the holes for the placement of implants and thermocouples. (b) Size of the implant.

Table 2. Chemical composition and mechanical properties of the consumables.

Chemical Composition (wt %)							
Consumable	**C**	**Si**	**Mn**	**Ni**	**Mo**	C_{eqIIW}	P_{cm}
ER 70S – 6	0,08	0,90	1,50	-	-	0,33	0,19
E 110 – MC	0,03	0,50	1,60	2,25	0,60	0,57	0,20

Mecanical properties				
Consumable	**Yield Strength (YS) MPa**	**Tensile Strength (TS) MPa**	**Elongation (ε) %**	**ChV (J) (-29ºC)**
ER 70S – 6	560	470	25	70
E 110 – MC	800	850	18	50

Equation (1) is known as the carbon equivalent parameter, parameter measurement set of crack or formula Ito-Bessyo. It is used in steels with carbon content below 0.12% and is suggested a value of Pcm ≤ 0.25%, for the purpose of obtaining better results weldability, minimizing the possibility of cracking. Equation (2) is known as carbon equivalent formula IIW. Was developed in the 40s for standard steels with high carbon content, however, by their wide application is still widely used. Values of Ceq (IIW) ≤ 0.45% indicates good metallurgical weldability of steels.

2.2. Acoustic Emission System - AES

For the analysis of the signals emitted by the crack was developed a acoustic emission system - AES, as shown in Fig.2(a). The system consists of four parts: (a) Set the system equipment trainers acoustic emission; (b) sensor (Fig.2(b)); (c) data acquisition board (A/D) (Fig.2(c)) and (d) computer interface. The developed set of equipment for the acoustic emission system developed consists of modules, which all were prepared on a printed circuit board: amplifying module signals; filter module "high-pass"; filter module “low-pass" and full wave rectifier module.

The feeding equipment and circuits that make up the AES is made by a regulated source designed to be supplied with a voltage of 127/220 VAC and an output voltage having symmetrical +15/-15 VDC to power the various modules the system. The sensor for the detection of cracks is based on the principle of piezoelectricity. This sensor, Panametrics M103 model, was designed for a center frequency of 1 MHz

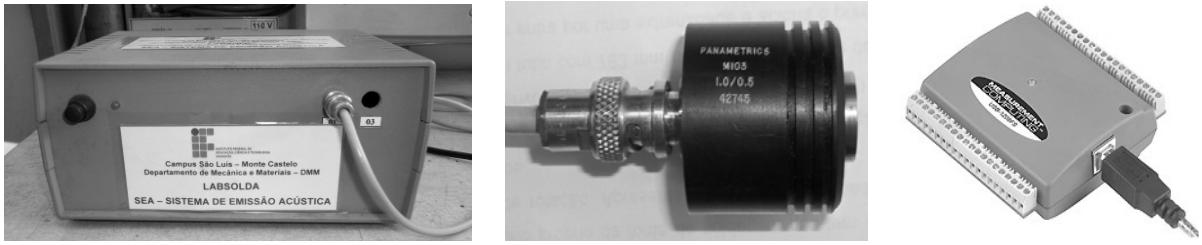

(a) (b) (c)

Figure 2. (a) AES; (b) Sensor; (c) Data acquisition board.

ISSN 2176-5480

Although the sign of the SEA treaty, it still cannot be entirely stored in the computer due to the limitation of its memory in relation to the large amount of data collected during test time (within 24 hours). Then, the computer program was developed to capture and store the data with a cutoff limit preset by the user. This caused the computer only stores all data related to crack propagation, ignoring the noises and values near zero. The system worked in the range of 0 to 10 V and the noise cut after preliminary tests, was 0.30 V. In Figure 3(a) you can see the main screen of the software. The software has a very simple interface and common to the software to work on Windows, because it was in Delphi 7.0 visual programming, which is compatible with Microsoft Windows operating systems versions 7.0, XP, NT and 2000.

In order to evaluate the sensor sensitivity and robustness of the whole system AES, initially put up the sensor connected to a steel plate and after the start of the acquisition were applied vibrations on the plate-shaped hit with a metal bar. Figure (3a) shows the signals obtained from the AE and Fig (3b) is shown an example of signals captured by the program without noise. Preliminary tests were carried out varying the signal line of cut from 0.20 V until reaching the signal considered ideal and was characterized as a set of crack signal. After performing all the preliminary tests, the signals below 0.30 V were classified as low-noise intensity level and was eliminated by cutting the tax software. All points earned below this value are not stored by the acquisition system. This value was determined after several preliminary tests, noting that this technique was also used in studies of Ferraresi (1996) and Fals (1999). For final testing line cutting the signal became 0.30 V. The acquisition rate was 2000 points/s for all the bodies proofs tested and recorded signals were found above 0.30 V, that is, above the noise level of the system AES.

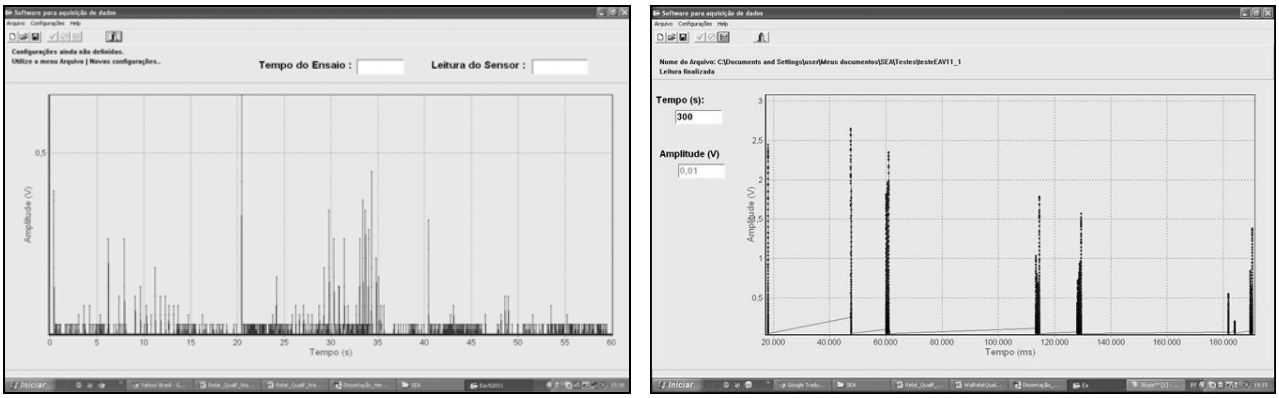

(a) (b)

Figure 3. Example screen showing signal captured by the program. (a) Noisy signals, (b) Signals without noise.

2.3. Implant Test

For the tests we used test equipment implant that is intended to evaluate the susceptibility to cracking by hydrogen. The equipment consists of two interactive systems: (a) a system of drift, consisting of a hydraulic system and the metal frame of the equipment, with the function of the traction of the body proof, simulating a state of internal stresses as seen in welded joints and (b) a monitoring system with the function of monitoring the strain relief, as well as the occurrence of cracking (breaking of (BP). Figure (4) illustrates, in schematic form, the implant test equipment of the welding laboratory of LAPROSOLDA/FEMEC/UFU.

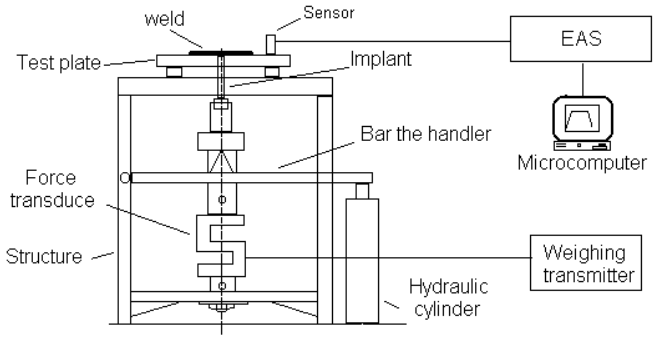

Figure 4. Implant equipment test LAPROSOLDA/FEMEC/UFU.

The test consisted of inserting the BP into an existing hole on the top of the testing machine, as shown in Fig. (5) and secured in the holder by tapping the plate and then with the hole for inserting the implant was placed in the BP assembly and inserted into this hole, so that the cutout portion BP of the hole plate to stay flush with the surface thereof.

ISSN 2176-5480

After mounting the plate BP in a weld bead 100 mm length was placed over the top plate through the hole, and thus the BP, at predetermined conditions, using consumable welding process and desired.

After welding and before the complete cooling of the weld occurred a constant tensile load was applied to the BP, imposing the same deformation. In the event of fracture, time to fracture of BP was determined. The tensile load applied was monitored by a load cell model Z-5T equipped with a strain gage sensitive to changes in applied force capable of transforming mechanical stress into an electrical signal and potential to measure up to five tons. A transmitter of the signal received from the weighing load cell and sent to analog/digital interface, showing the intensity at a given instant of the request via a digital indicator.

Before the start of the test there was a cleaning of the hole in the sheet BP insertion with acetone and BP by ultrasound. After welding, monitored the temperature recorded at the thermocouple until it reached 150°C, Fig. (6). Then, the load was removed from the hydraulic system then being gradually traction applied on the BP. Thus the BP has to be subjected to a pure tensile stress constant throughout the test. Was placed on the test plate the thermocouples, AE sensor and began signal acquisition for 24 hours or until breakage occurred implant.

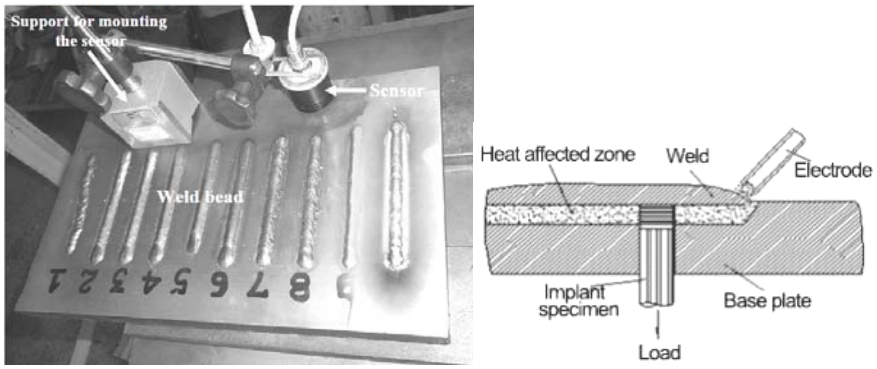

Figure 5. Fixation of the implant in the test plate (plate insertion of the implant).

2.4. Analysis of the specimens

The BPs tested and not fractured were analyzed with the results presented by AES. With the signals obtained was possible to prove the existence of the crack and the result of the acquisition of the acoustic emission sensor demonstrate the feasibility and sensitivity of AES in crack detection of hydrogen. The BPs tested who fractured were analyzed using the results presented by the AES and the behavior of the mode of fracture at the tip of the implant. Thus, it was possible to relate the results of the acquisition of acoustic emission sensor and the fracture mode and prove the feasibility and sensitivity of AES in crack detection of hydrogen

3. Results and Discussions

In the Table 3 can be seen the results of tests with different energies welding and applied loads, where the variables are related to the test implant C_i, C_f, T_f and variables resulting from data acquired by the AES are tpi, tpf, vp, np.

Where:

Ci - initial load registered by the load cell in the implant (kgf);

Cf - end load registered by the load cell in the implant (kgf);

Tf - Final temperature at the instant of rupture or not the specimen (C);

tpi - Time of the first excitation (peak) recorded by the AES (ms);

tpf - Final time registered by AES on break or not the specimen (ms);

vp - value greater arousal (maximum amplitude) registered by the AES (V);

n_p - Number of excitations (peaks) stored above the cutoff limit throughout the test.

Forces applied on the implants

The stresses shown in Tab.3 were calculated considering the requests as axial traction. In calculating the area was regarded as the external diameter of the implant (6 mm), since the groove (thread) is regarded as a defect in the total area of triaxialidade causing tensions in the region, whether the tip of the implant has no notch sharpness required to obtain a pre-crack as defined by fracture mechanics theory. The area used was 28.27 mm^2. The stresses applied to the implants had by reference to the recommendation of standard AFNOR NF-89 100 (1991). This standard is set to use 80% of the yield strength of the material as critical stress being applied to fracture the material. According to NF-89 100 This percentage corresponds to the stress where no cracking occurs in the implant after application of the load in the first 16 hours of the test. In this work random loads were applied for a period of 24 hours, until it appeared to fracture or not, and then compared with the recommendation of standard AFNOR NF-89 100. To evaluate are considered the stresses applied loads initially seen that after this, in the case of the implants ruptured, there is a reduction in tension as

ISSN 2176-5480

a result of the elongation of the material and showing its ductility cannot be recorded by the equipment available. The final load corresponds to the instant of rupture. From Table 3 it can be seen that only the implants stress greater than 75% of the yield strength broke BP. It is also observed that implants soldiers with hydrogen in the composition of the shielding gas broke with lower stress applied to the other. This is due to the effect caused by hydrogen added to the shielding gas that weakens the welded joint and agrees with the results presented by Falls (1999). Although this table highlights that loads initially applied in welded cored wire implants were bigger than welded with solid wire, this is due to the fact that the tubular wire has superior mechanical strength to the solid wire.

The analysis of the results shown in Tab.3 which is observed in the implants that did not break after application of the initial and after the test due to problems of expansion and flow of the material, the final value of this force is different from that of initially, and as there was no the breaking of the implant, it remained constant until the end of the test. Under these conditions, the applied loads were lower than the applied loads on implants that ruptured and therefore it can be said that this fact may have contributed to not break them. Even in the implants showed signs that the AES and not broken (I2, I4), the applied loads were lower than those applied in the implants ruptured, showing its influence.

Table 3. Results of tests implants

Test	E (Kj/mm)	Gas	C_i (Kgf)	C_f (Kgf)	T_f (ºC)	t_{pi} (ms)	t_{pf} (ms)	v_p (V)	n_p
Cored Wire (AWS 5.28 E 110 MC)									
I1*	1,0	A	1290	1300	Amb	-	-	-	-
I2[2]			1385	1410	Amb	6415664,5	$172,8x10^6$	4,76	1
I3[1]		B	1467	1395	40	853542,5	853656	9,98	5
I4[2]			1400	1409	Amb	11408442,5	$172,8x10^6$	4,95	3
I5*	1,5	B	1325	1338	Amb	-	-	-	-
I6[1]			1473	1425	56	1995000,5	1995092	9,61	4
I7[1]			1487	1413	59	349027,5	349196,5	9,98	3
I16*		A	1330	1340	Amb	-	-	-	-
Solid Wire (AWS 5.18 ER70S-6)									
I8[1]	1,0	B	1445	1300	48	782868	782895	9,76	1
I9[1]			1450	1320	47	1067511	1067523	9,98	3
I10*		A	1410	1417	Amb	-	-	-	-
I14*			1401	1413	Amb	-	-	-	-
I11*	1,5	B	1352	1360	Amb	-	-	-	-
I12[1]			1444	1387	54	671427,5	671488,5	9,98	3
I13[1]			1453	1372	47	1442123	1442338,5	9,98	5
I15*		A	1340	1360	Amb	-	-	-	-

Symbols: E = Energy generated in arc welding, **Gas A** = Ar + 25% CO2; **Gas B** = Ar + 15% CO_2 + 3% H_2; **Amb** = Ambient Temperature; ***** = Specimen not broke; **1** = Body proof that broke; **2** = Specimen not broke more signal presented in AES.

Results of the specimens not fractured and not signed at AES

Analysis of the results presented in Tab.3 note that the samples I1, I5, I10, I11, I14, I15 and I16 did not break and showed no sign in AES. However, even under these conditions, these specimens were examined metallographically and crack was not detected. This fact may be related to the low stress level applied and the diffusivity of hydrogen in conditions that were soldiers. Exception occurred at implantation I10, Fig.6, that after the optical microscopy showed the existence of a crack in the notch of CGHAZ. According to Tab.3 this implant was subjected to an initial load of 1410 Kgf and after expansion and cooling does not exceed the load of 1417 kgf. The crack was not detected by the SEA because of its size, this because at the time of its beginning it has not generated an amplitude above the noise levels of the system (0.30 V). The behavior shown in Fig.6 the crack is in CGHAZ exactly in the notch and consequently this is a hydrogen crack.

Results of the specimens not fractured and with sign in the AES

The I2 specimen was welded under the conditions shown in Tab.3 an 150ºC the test was started. After the lapse of 107 min AES recorded a peak and the specimen did not break. At the time of the signal specimen was at a temperature of 40°C. In accordance with the signal captured by the AES the maximum amplitude recorded for this peak was 4.76 V. Analyzing the evolution of the signal captured, it had a duration of 26 ms and the initial time was in 6415664.5 ms (106.92 min) and final 6415690.5 ms as identified in the program screen and shown in Fig.7a. This peak shows a start behavior of a crack in the specimen.

ISSN 2176-5480

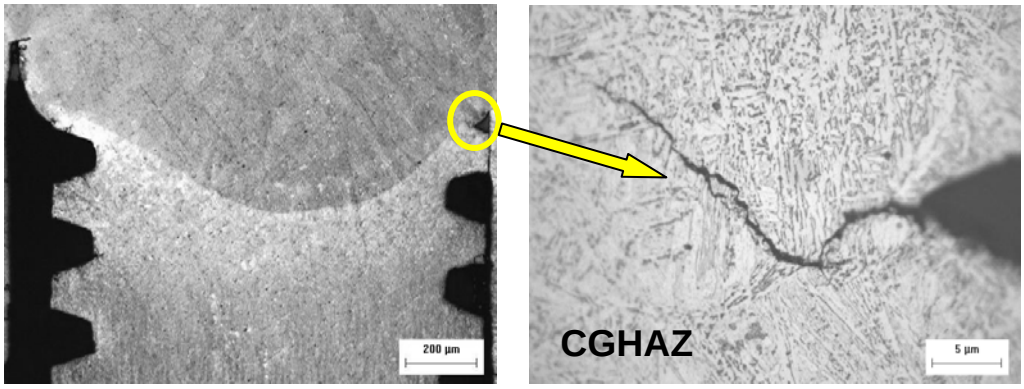

(a) (b)

Figure 6. Detail of the implant I10. (a) macrograph showing that the implant has not ruptured (37.5 X);(b) detail of the crack in the notch in the hydrogen CGHAZ (1500X).

The I4 welding conditions are shown in Tab.3 and the start of the trial occurred when the temperature reached 150°C. After the lapse of three hours (180 min) the AES recorded the first peak and the specimen did not break. At this time the specimen was already at room temperature. For this test were recorded three peaks. According to the signals captured by AES, Fig.7(b), the maximum amplitude recorded occurred at the peak (1) was 4.95 V and had a duration of 27 ms. Analyzing the evolution of other signals captured by AES during 11408442.5 ms to 11430984.5 ms from the beginning of the trial and identified on the program screen shown in Fig.7(b), it is possible to verify that the first peak indicates it is the early formation of hydrogen cracking. The second peak (2) occurred in 11408668 ms (3.74 V) with duration 19 ms indicating the crack propagation, the third peak (3) at 11430962.5 (4.34 V) lasting 22 ms also indicates crack propagation. Having been a soldier I4 with hydrogen in the composition of the shielding gas and more the action of the applied load these may have contributed to the crack occurred and its propagation, however, the diffusion of the hydrogen, crack propagation did not occur in order to bring the specimen to rupture. Figure 8(a) and 8(b) shows optical microscopy (OM) of the implant I2 and I4 respectively and the presence of a crack in the region of the coarse grain HAZ (CGHAZ), confirming that the signal obtained for AES corresponding crack hydrogen.

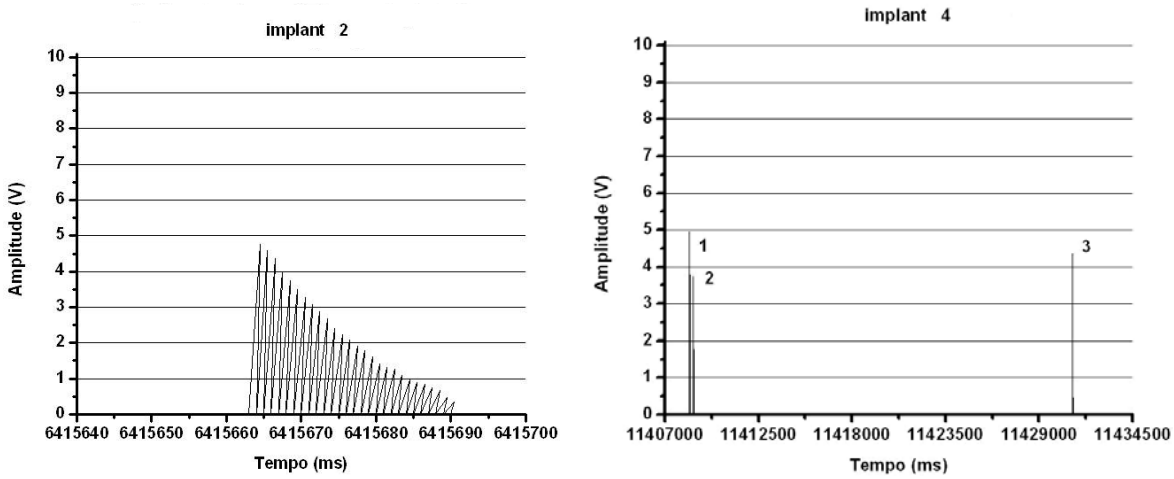

(a) **(b)**

Figure 7. (a) Signal captured by the AES to I2. (b) Signal captured by the AES to I4.

It is observed in Fig.8 that the crack formed in the HAZ zone fragile due to grain growth, microstructural changes and the effect of triaxial stress-induced notch implant inserted in this region. The crack appears transversely to the HAZ growing toward the weld zone (FZ). The appearance of crack hydrogen is due to the high hardness in this region and also due to the microstructure of martensite and bainite present in typical steels API X80. Note also that in the transition region ZTA / ZF appears a discontinuity that probably should have been responsible for relieving the stress and thus prevent further spread of the crack until failure.

Results of the specimens fractured and sign in SEA

In the Table 3 can be seen the welding conditions of ruptured implants and the temperature of the beginning of tests took place at 150°C. To implant I3 have passed 14.2 minutes after the start of the test the specimen broke at 40°C. For this test were registered 5 peaks. According to the signals captured by the AES, Fig.9(a), there is, for decreasing behavior of the load, the material deformed before rupture occurred, and only after the signal has reached an amplitude

ISSN 2176-5480

of 9.98 V the specimen fractured. Analyzing the evolution of the signals during 853542.5 ms to 853692 ms of the start of the test and identified on the program screen shown in Fig.9(a), it is possible to verify that the first peak occurred at 853542.5 ms (14,2 min) from the beginning of the test, reached an amplitude of 4.03 V and a duration of 21.5 ms with a decay characteristic wave AE and indicating it is the beginning of the formation of hydrogen cracking. The second peak (2) began to 853570 ms (1.89 V), duration of 12 ms and the third peak (3) to 853584.5 (0.68 V), duration of 6 ms, show a behavior of crack propagation. The fourth peak (4) happened at 853600 ms (0.49 V), duration 4 ms may be interpreted as the end of the crack propagation. The peak (5) 9.98 V occurred at 853642.5 ms with a duration of 49.5 ms is the final instant of rupture of the CP, resulting in impact the BP with the equipment structure, generating a signal high intensity (break CP). This behavior was found in all specimens that fractured.

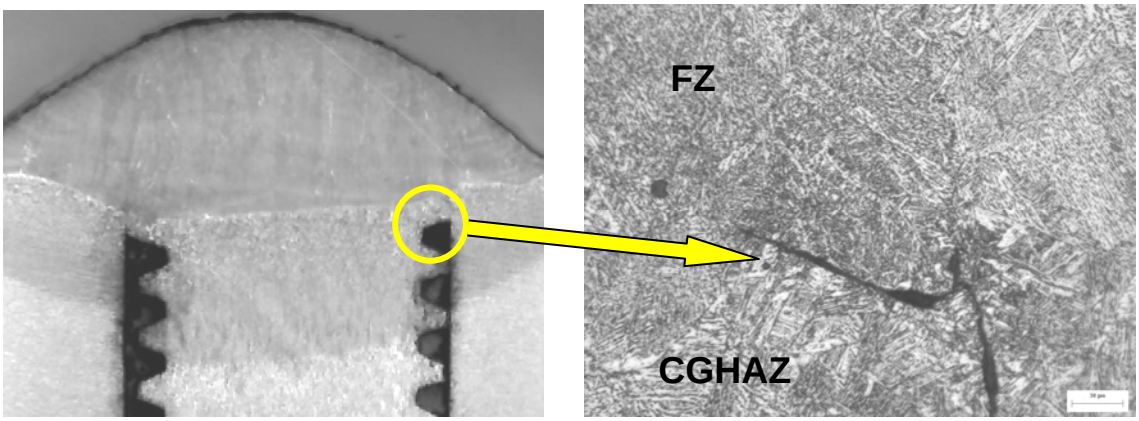

(a)

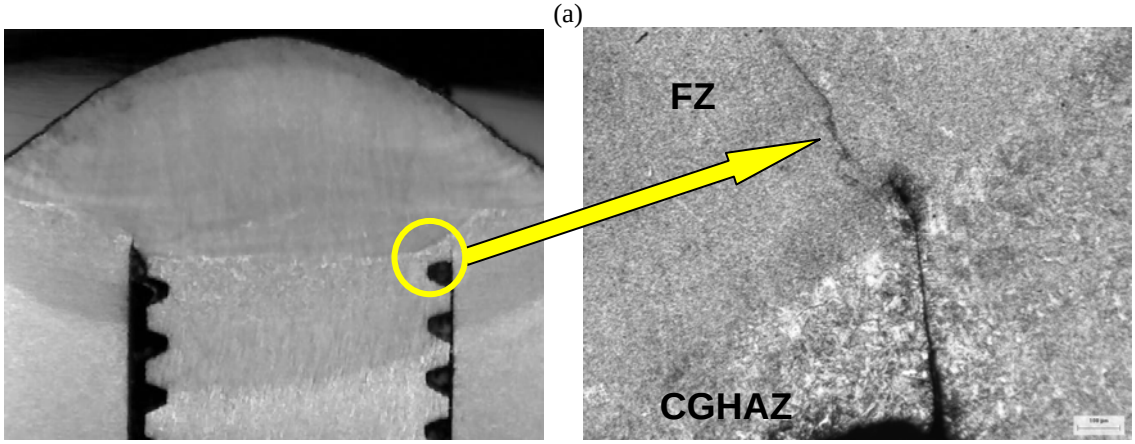

(b)

Figure 8. (a) Detail of the implant I2. Macrography showing that the implant does not ruptured (37.5 X) and detail of the crack hydrogen in the CGHAZ (300X); (b) Ditto for the implant I4.

The implant I6, after 33,25 min have passed 33,25 min the specimen broke at 56ºC. For this test were registered 4 peaks. There is, by the behavior of the load, the material deformed before breaking as occurred with I3. The progression of the signals captured by AES during 1995000 ms to 1995100 ms of the start of the test and the program identified in the screen shown in Fig.9(b), it is possible to verify the peak and the first peak occurred at 1995000.5 ms, reached an amplitude of 1.64 V and lasted 12.5 ms indicating it is the beginning of the formation of hydrogen cracking. The second peak (2) occurred at 1995050.5 ms (0.69 V), duration of 9 ms indicating the crack propagation, the third peak (3) to 1995066.5 (0.69 V) with duration of 10 ms, as described above, can be understood as the end of the crack propagation hydrogen. The behavior of the fourth peak (4), 9.61 V, occurred to 1995079 ms and duration of 42 ms is the final instant of rupture of the BP, resulting in impact to the BP with equipment structure, generating a high signal intensity as already described for the I3 and common behavior in fractured implants.

The I7 implant ruptured after the lapse of 5.8 min at 59ºC. For this test were registered three peaks with intensity above 0.30 V. Analyzing the evolution of the signals captured by EAS during 349027.5 ms to 349196.5 ms from the beginning of the trial and identified on the program screen shown in Fig.9(c), it is possible to verify that the first peak occurred in 349027.5 ms, reached an amplitude of 3.6 V and lasted 21 ms indicating it is the beginning of the formation of hydrogen cracking. The second peak (2) occurred at 349055.5 ms (4.97 V) with duration of 25 ms indicating crack propagation. The behavior of the third peak (3) 9.98 V occurred on 349196.5 ms, duration 55 ms and can be explained as described above.

As seen in Fig.9, the behavior tendency of the signals captured by the AES in tests with core wires is the same. Initially arise low amplitude signals followed by others until a very high amplitude characterizing the instant of rupture

ISSN 2176-5480

of the implant. This behavior can be explained by Lee, *et al* (1999). According to the author in the region of the joint most events EA is associated with the movement of dislocations during the strength of the material only a single peak EA, consisting of low power event is found around that point. In the HAZ and ZF together with the first peak, a second peak (and other) consists of the events high energy appears in the post-strength and are presumed to be associated with the occurrence of microcracks in the interface ferrite/martensite and/or within the martensite. The behavior of AE steel heat treated with different amounts of martensite is also characterized by the existence of a second (or other) peak EA. Both the amplitude AE and the number of events increases as the volume fraction of martensite increases. The cracks are found in the interface ferrite/martensite and/or inside the martensite. In the case of deformation of ferrite matrix, the AE shows a signal waveform rise time long length and small amplitude, and the peak of the frequency spectrum occurs at a relatively high frequency (~ 170kHz). However, when cracking occurs interfacial ferrite / martensite waveform is characterized by a short rise time and a high order of magnitude aplitude than the first frequency and peak occur at a low frequency (~ 110 kHz).

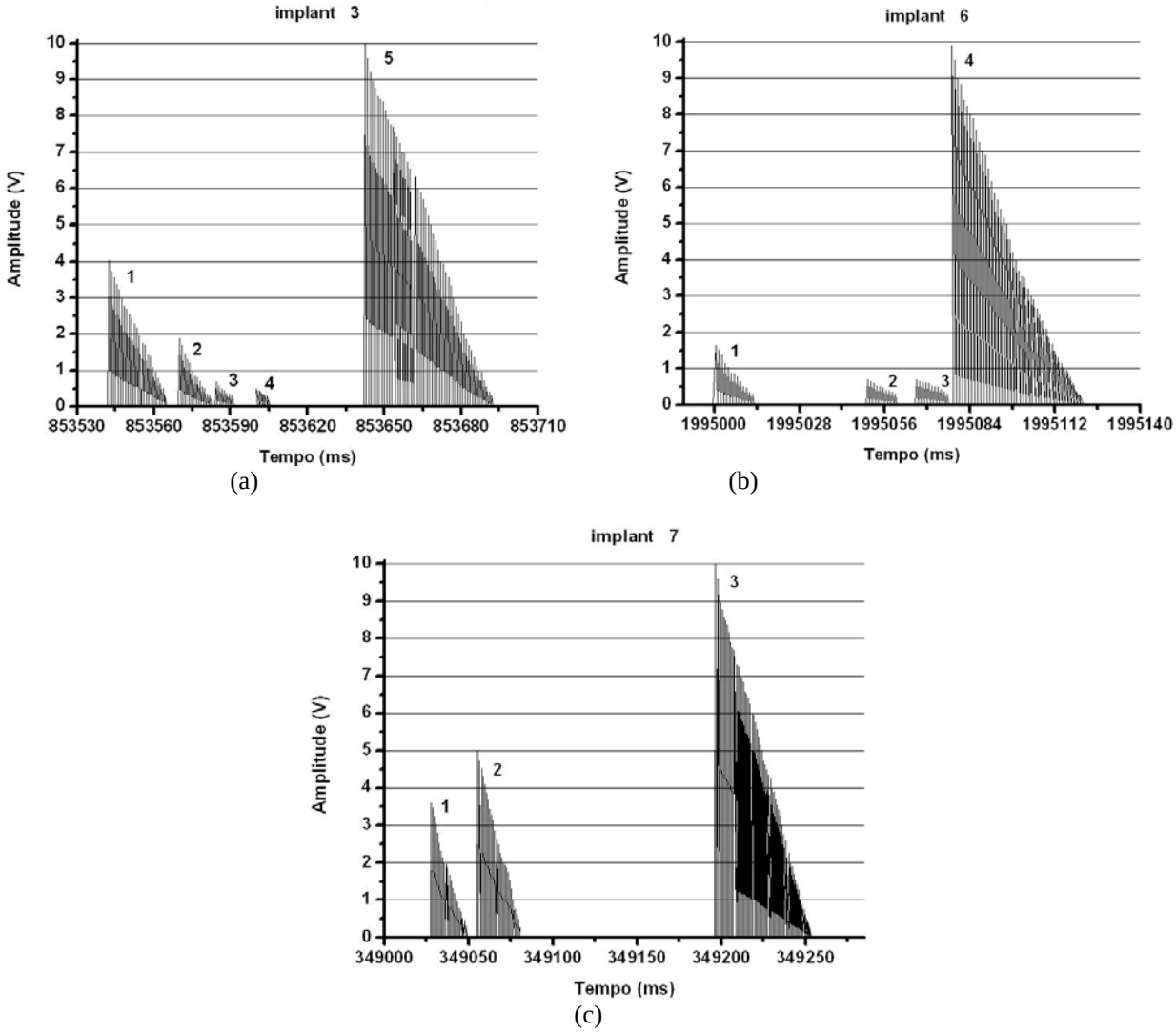

Figure 9. Signal captured by AES for I3, I6 and I7 welding with cored wire and shielding gas Ar + 25%CO_2 + 3%H_2. Welding energy 1.0 kJ/mm (I3) and 1.5 kJ/mm (I6 and I7).

As can be seen in Fig.10, the behavior tendency of signals captured by AES in the other solid wire testing are similar to the test performed with cored wire with respect to the behavior of the signals. As in welding with cored wire, there are low amplitude signals followed by the other up to a high amplitude characterizing the instant of rupture of the implant. This behavior is the same as explained above. The results obtained by the SEA shows that steel when welded under the conditions provided in this work shows sensitivity to the formation and propagation of cracks hydrogen, which was higher in the tests with the addition of hydrogen in the shielding gas and the behavior of the signals is closely related to the microstructure resulting from welding. Microstructure with large grain growth of primary austenite and martensite can influence the type and waveform AE obtained, explains Lee, *et al* (1999).

ISSN 2176-5480

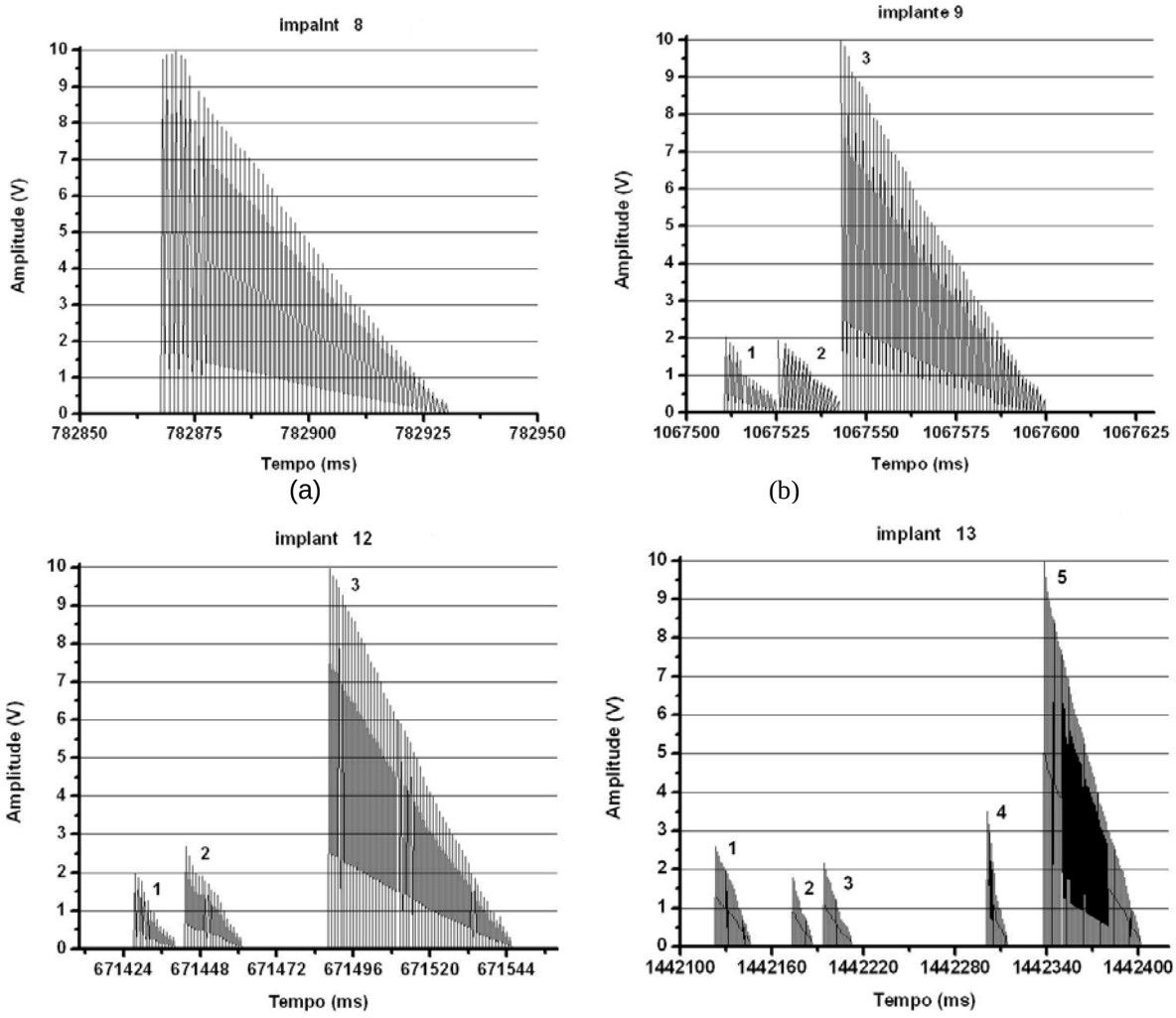

Figure 10. Signal captured by AES to I8, I9, I12 and I13 weiding with solid wire and shielding gas Ar + 25%CO_2 + 3%H_2. Welding energy 1.0 kJ/mm (I8 and I9) and 1.5 kJ/mm (I12 and I13).

Microfractographic investigations

For a detailed examination of hydrogen cracking, the fracture surfaces of implant specimens were examined using SEM technique. Some typical microstructure regions observed under the microscope are shown in Fig. 11. We know that the propagation of crack occurred both transgranularly and intergranularly. It should be noted that in bainite or martensite structure cracks run only transgranularly. Figure 11 shows examples of microfractografs, where the majority of the fracture surface shows dimples pattern. However, the decrease in applied stress had a tendency to increase the quasi-cleavage affected by hydrogen. Exceptionally, near the notch, intergranular fracture surface was observed.

In evaluating Matsuda, *et al* (1978), the presence of hydrogen and allowable stresses of the order of 50 Kgf/mm^2 the fractured region shows intergranular fracture area and the area of fracture dimples, indicating a fracture caused by crack hydrogen. The micromechanisms of fracture dimples represent the behavior of ductile fracture. Occurs by nucleation, growth and coalescence of microvoids. The growth of voids and the deformation is controlled by coalescence occurs necking inner end of the ligaments between the voids. The dimples fracture usually occurs through the grain. These fracture modes vary in their extent and distribution dependence on the applied stress and the presence of hydrogen (derived shielding gas) agreeing with the "Theory of Plasticity Due to Increased Hydrogen Located" proposed by Beachem and developed by Birnbaum et al in 1997.

In the region of crack initiation, Fig.11(a), there is coalescence of micro voids (CMV). According Fals (1999), this characteristic is due to the fact that the radius of curvature of the initial notch in the implant is large compared to the radius of the crack tip that propagates and shape, resulting in less stress concentrator, however, facilitating the formation of CMV, even in the presence of an increased brittleness as a result of the excess of hydrogen within the material. After that, the crack grows when the sharpness of the tip and thus increases stress concentrator increases, thus causing the transition to the fracture mode of quasi cleavage (QC),Fig.11(d). The transition from CMV to QC is faster when there is an increase in the applied stress, in agreement with the data of this work since the stress applied to the implants ruptured were higher than I2 and I4 already analyzed. Thus, for the implants welding with hydrogen in

ISSN 2176-5480

shielding gas and higher stress applied, the plastic zone at the crack tip was lower, probably due to the effect of stacking disagreements, causing the increase in the QC mode fracture surface of the implant .

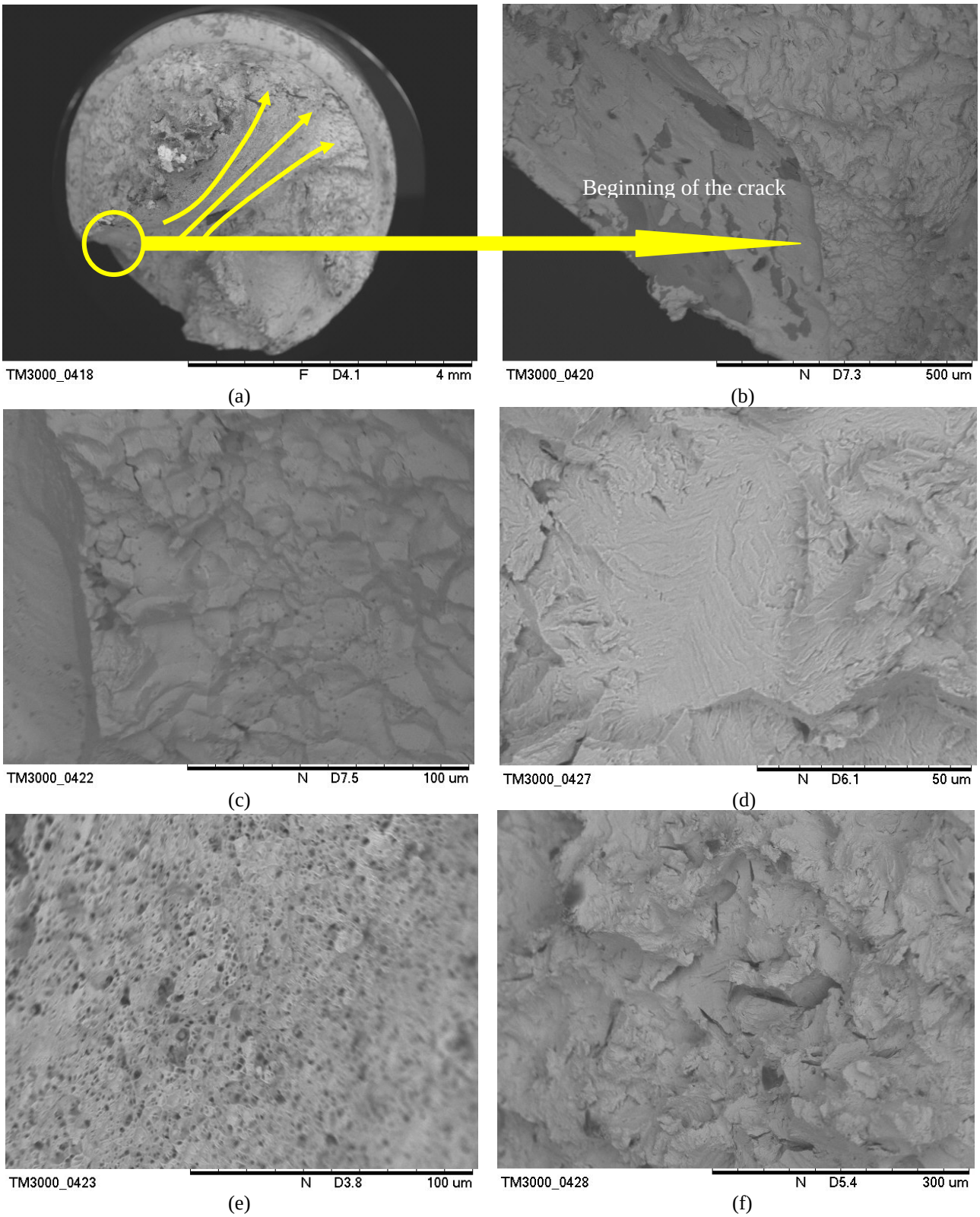

Figure 11. Typical microfractografia presented by implants. (a) The tip of the implant, (b) Detail fracture initiation region. (c) and (d) Detail of the fracture in the region of a crack, intergranular and transgranular respectively; (e) Detail the dimple region (f) Detail of the break region of material.

ISSN 2176-5480

3. CONCLUSIONS

• With the signals obtained by the AES was possible to prove the existence of the hydrogen crack and the result of acquisition of the acoustic emission sensor prove the feasibility and sensitivity of the detection system of this kind of crack.

• Through the use of the implant test, within the welding conditions in this work, we found that the broken hydrogen occurring in the HAZ and in the weld zone which is due appearance of microconstituents susceptible in the weld microstructure.

• the hydrogen cracking occurred more frequently during the first hour of the test, having had the lowest occurrence time of 5.8 minutes and the longer 3 hours after the test and the final temperature below 60°C.

• The BPs weldings with solid wire and cored wire, provided 1.0 and 1.5 kJ/mm welding energy and hydrogen in the composition of the shielding gas fractured. Exception is made in BPs I2 and I3 that were welded with FCAW, energy of 1.0 kJ/mm, with and without hydrogen in the composition of the shielding gas respectively, not fractured, but showed signs detected by AES.

• The fracture surface morphology showed a mixed fracture presenting as much cleavage fracture and intergranular ductile fracture. Almost all fractures occurred at ZTA or near the fusion line. The fracture occurred in the region near the fusion line extended to the HAZ and in other cases the interface HAZ/BM. Particularly for the notch in the HAZ, the cleavage fracture shows the action of hydrogen as an embrittled material.

4. ACKNOWLEDGEMENTS

To CAPES for funding this research studentship, the Usiminas for providing the base material, the LAPROSOLDA / FEMEC Federal University of Uberlândia / UFU and the Federal Institute of Maranhão / IFMA for supporting this work.

5. REFERENCES

Boellinghaus, T., Viyanit, E., Zimmer, P., 2010. “Cold Cracking Tests” .Revision, IIW – Doc. Nº II-A- 111.03-Revision6. Disponível em http://www.china-weldnet.com/English/ information/ II-1587-06.htm. Acessado em 05 de abril de 2010.

Fals, H. D. C. 1999. “Proposta de um Ensaio para Avaliação das Trincas Induzidas por Hidrogênio em Juntas Soldadas Assistida por Emissão Acústica”. Universidade Estadual de Campinas, 1999. 203 p. Tese (Doutorado).

Ferraresi, V. A. 1996. “Estudo do fenômeno Trinca de Reaquecimento com auxílio da Emissão Acústica”. Tese, Universidade Estadual de Campinas, Campinas, SP 173 p, 1996.

Hippsley, C.A., et al., 1988. “A study of the Dynamics of High Temperature Brittle Intergranular Fracture By Acoustic Emission”. *Acta Metallurgica*, V.36, n.2, p.441-452

Lee, C.S, et al., 1999. “Acoustic Steel Emission Behavior Welds During Tensile Test of Low Carbon”. *ISIJ International*, V.39, n.4, p.365-370.

Matsuda, F. et al. (1978). “Effect of hydrogen content on cold crack susceptibility of various steels with the implant test”. *Transactions of JWRI*, Vol. 7, nº 1, pp. 47-53.

Nevasmaa, P., 2003. “Predictive model for the prevention of weld metal hydrogen cracking in high-strength multipass welds”. Department of Mechanical Engineering, University of Oulu, P.O.Box 4200, FIN-90014 University of Oulu, Finland Oulu, Finland, 2003.

Widgery, D. J., 2002, “High strength weld metals – routes for development”, IIW Doc. II-1459-02.

6. RESPONSIBILITY NOTICE

The authors are the only responsible for the printed material included in this paper.